Carbon anode materials for lithium ion batteries

Y.P. Wu[a,b,*], E. Rahm[b], R. Holze[b]

[a]*Division of Chemical Engineering, INET, Tsinghua University, Beijing 102413, China*
[b]*Elektrochemie AG, Institut für Chemie, Technische Universität Chemnitz, 09107 Chemnitz, Germany*

Abstract

Since the birth of lithium ion battery in the end of 1980s and early 1990s many kinds of anode materials have been studied. Nevertheless, graphitic carbon is still the only commercially available product. As a result, modification of carbonaceous anode materials has been a research focus. In this paper, latest progress on carbon anode materials for lithium ion batteries is briefly reviewed including research on mild oxidation of graphite, formation of composites with metals and metal oxides, coating by polymers and other kinds of carbons, and carbon nanotubes. These modifications result in great advances; novel kinds of carbon anodes will come in the near future, which will propel the development of lithium ion batteries.
© 2002 Elsevier Science B.V. All rights reserved.

1. Introduction

Since the technological breakthrough of anode materials for lithium secondary battery in the end of 1980s and early 1990s resulting in the birth and commercialization of lithium ion battery, research on anode materials has been a focus. So far, a lot of anode materials has been investigated including graphitic carbon, amorphous carbon, nitrides, tin oxides and tin-based alloys [1]. However, to our knowledge graphitic carbon is still the dominant one available on the market; this indicates the importance of carbonaceous anode materials. There are a lot of reviews about carbon anode materials [1–3]. However, with the progress of technology new aspects concerning modification and preparation of carbon anode materials have appeared. Here, we review the latest progress of research on carbon anode materials, mainly including mild oxidation of graphite, formation of composites with metals and metal oxides, coating with polymers and other kinds of carbons, and carbon nanotubes.

2. Mild oxidation of graphite

It was first reported by Peled et al. that mild oxidation of artificial graphite could modify its electrochemical perfor-

mance as anode material for lithium ion batteries [4]. The main effect is ascribed to two processes: the production of nanochannels and/or micropores and the formation of a dense layer of oxides. The former enhances lithium intercalation [5], and the latter inhibits the decomposition of the electrolyte. As a result, reversible capacity and coulomb efficiency in the first cycle increase. But, it should be born in mind that the oxidation should not be drastic. If graphite is over-oxidized, an opposite effect will be observed [4]. Later, other graphitic materials and oxidation agents such as ozone and carbon dioxide were investigated [6–10], and similar improvements have been achieved. However, the degree of improvement is different depending on the used graphite material. Metals or metal oxides can be introduced to favor this oxidation process and more nanochannels/micropores can be introduced. In addition, the metals can perhaps act as sites for lithium storage. As a result, reversible capacity is further enhanced [11].

Oxidation can also be used to modify electrochemical performance of high-temperature treated graphite [12]. High-temperature treatment of a highly crystalline synthetic graphite, TIMREX® SLX50, under inert gas atmosphere leads to an increased crystallinity with no evidence of rhombohedral stacking defects in the hexagonal graphite crystal structure as well as a significantly lower specific BET surface-area. Solvated lithium ions can co-intercalate therein causing significant exfoliation of the graphite sheets and increase of irreversible capacity. In order to circumvent the exfoliation, an additional oxidation treatment of the

heat-treated TIMREX® SLX50 in air has been tried. This oxidation produces a surface curing effect, increases the amount of disordered carbon atoms and the oxygen atom concentration as well as the amount of prismatic surfaces, but keeps the number of low-energy defects unchanged. Due to these changes in surface structure, co-intercalation of solvated lithium ions vanishes at oxidation temperatures above 800 °C [12], and significant improvement in cycling behavior will be achieved.

In the case of practical application this oxidation method has a shortcoming, i.e. the reproducibility and uniformity of products cannot be well controlled since this oxidation happens at the interface between the solid and the gas phase. Consequently, liquid oxidants have been explored and good results have been achieved [13–18]. For the first time, we found that defects such as sp^3-hybridized carbon atoms, carbon chains and carbon radicals in common natural graphite could be removed by oxidation. As a result, the stability of the graphite structure is improved. This oxidation produces additional micropores and nanochannels and forms a dense layer of oxides on the graphite surface. Consequently, electrochemical performance including reversible capacity, coulombic efficiency in the first cycle and cycling behavior improves markedly. In contrast, prior to oxidation treatment, reversible capacity is only 251 mAh/g, and it fades to 105 mAh/g in the first 10 cycles. An aqueous solution of $(NH_4)_2S_2O_8$ has the strongest oxidation ability (standard oxidation potential: 2.08 V) among stable liquid oxidants. This method provides material with the highest stable reversible capacity up to 355 mAh/g [15]. The oxidation ability of concentrated nitric acid solution (the highest standard oxidation potential among its decomposition products is 1.59 V) is lower than that of $(NH_4)_2S_2O_8$. Nevertheless, it still produces similar improvement [16]. One disadvantage of these two solutions is that they are not friendly to the environment. Green chemistry has been a focus due to urgency of environmental protection. The standard oxidation/reduction potential of $Ce(SO_4)_2$, 1.61 V, is a little higher than that of nitric acid and lower than that of $(NH_4)_2S_2O_8$ [17]. Therefore, it has been tried as a green oxidant to modify the electrochemical performance of natural graphite. However, it will result in some corrosion of equipment due to introduction of a salt. Later, a solution of H_2O_2 (standard oxidation potential: 1.78 V) has been identified also as an effective oxidation agent, and a salt-free green method has been realized [17,18]. The unique characteristic of the treatment by soluble oxidants is that the treatment temperature is low (≤60 °C) and homogeneity of the product can be controlled easily since the reaction takes place at the interface between liquid and solid phases. A pilot plant shows promise for these methods [13], and part of these results are shown in Fig. 1 [14].

As mentioned major processes during mild oxidation can be summarized as following: (1) removing some active sites and/or defects in graphitic materials resulting in improvement of surface structure; (2) forming a dense layer of oxides acting as an efficient passivating film; and (3) producing
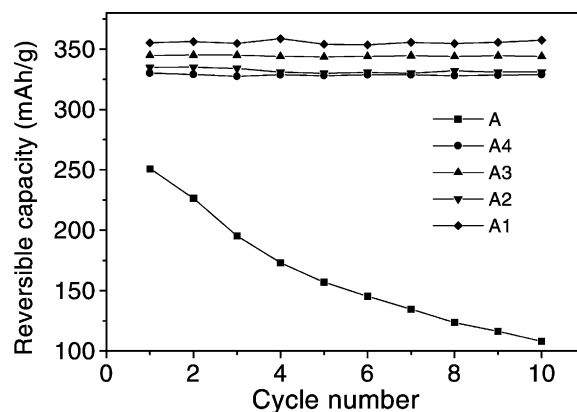

Fig. 1. Comparison of cycling behavior of one common natural graphite (A) before and after oxidation treatment by solutions of $(NH_4)_2S_2O_8$ (A1), HNO_3 (A2), $Ce(SO_4)_2$ (A3) and H_2O_2 (A4) at 60 °C (from [14]).

nanochannels/micropores for storage sites and passages for lithium. It is anticipated that these kinds of effects will also act on low temperature (non-graphitic) carbon, and thus improvement in coulomb efficiency in the first cycle and cycling behavior will be achieved.

3. Forming composites with metals and metal oxides

Silver has been first introduced onto the surface of graphite by composite formation [19,20]. Due to the increase of conductivity and the incorporation of additional lithium storage sites the rate capability and cycling behavior are much improved.

In order to suppress co-intercalation of solvated lithium ions into graphite, graphite is microencapsulated with nano-sized Ni to form composite particles. The composite shows great improvement in charge–discharge performance, coulombic efficiency, and cycling behavior as measured with a propylene carbonate (PC)-based electrolyte. For example, a 10 wt.% Ni-coated composite increases the initial charge–discharge coulomb efficiency of SFG75 graphite (75 μm, Timcal America) from 59 to 84% and the reversible capacity by 30–40 mAh/g. The Ni-coated composite consists of nanosized Ni particles distributed over the graphite surface. This coating blocks effectively some of the edge surfaces from exposure to the electrolyte and minimizes co-intercalation of solvated lithium ions at these edge sites, subsequent reduction of PC and exfoliation of the graphene layers. As a result, both the charge–discharge performance and safety of the negative electrode in a rechargeable Li-ion cell are improved [21]. In the case of KS10 graphite, this kind of coating also shows that the charge-transfer resistance (exchange current), surface film resistances, and lithium ion diffusion coefficient as functions of the state of charge (SOC) of the 10 wt.% Ni–graphite (KS10) composite are all improved as compared to bare KS10 graphite. The charge-transfer resistances are always lower, the respective exchange currents are larger by 26 and 27%, with an increase

from 137 to 614 mA/g as the SOC increases. The surface film resistances for the composite are slightly smaller, and the lithium ion diffusion coefficients are always slightly larger, ranging between 1.09×10^{-9} and 6.7×10^{-9} cm^2/s, than those for bare KS10. The composite exhibits less capacity loss over a 10-day storage period in comparison with bare KS10 [22]. Of course, other kinds of methods can also introduce nanometer Ni particles onto the surface of graphite such as hydrothermal hydrogen reduction [23]. Due to lower electron transfer resistance, its high rate capability is improved.

Tin can also form composites with graphite since it can be host for lithium storage [24–26]. When Sn is supported on large surface-area synthetic graphite (KS6) to obtain composite materials, an improved electrochemical performance relative to bulk Sn is observed. In general, the composites are superior to the mechanical mixtures of KS6 and Sn of similar overall composition in many performance aspects. The Sn–KS6 composites increase the reversible capacity of graphite at some expense of the cyclability. However, Sn could also contribute to the irreversible capacity loss in the first cycle, probably through a mechanism similar to the formation of a solid electrolyte interface (SEI) on carbonaceous surfaces [25].

Using an autocatalytic deposition technique tin-graphite composites can also be prepared. Electrochemical performance of the composites strongly depends on the amount of tin loading and the heating temperature. Heating the composite converts Sn from the amorphous into the crystalline form. Apart from higher capacity, Sn–graphite composites possess higher coulombic efficiency, better rate capability, and longer cycle life than the bare synthetic graphite [26].

When activated carbon fiber is coated by tin and its oxides through impregnation and following heat-treatment, the formed composite also shows enhanced capacity in comparison with the pure carbon [27]. When the amount of Sn is adequate, a good cyclability is achieved [27]. Nanosized particles of tin alloys such as SnSb, $Sn_{65}Sb_{18}Cu_{17}$ and $Sn_{62}Sb_{21}Cu_{17}$ can also form composites with carbon [28, 29]. In the case of composite of SnSb and MCMB, when the ratio of SnSb alloy is below 30 wt.%, the aggregation of nanosized alloy particles is alleviated, and its cycling behavior is improved with a high stable capacity up to 420 mAh/g [28]. Composites of nanosized (<100 nm) particles of $Sn_{65}Sb_{18-}Cu_{17}$ and $Sn_{62}Sb_{21}Cu_{17}$ with graphite show that lithium can be fully de-inserted from the host matrix only when the anode is cycled at low current densities. The kinetics of lithium insertion to and de-insertion from the composite anode materials slows gradually with the cycle number since the deposited alloy becomes amorphous during cycling though the graphite does not. Consequently, the active materials in the composites suffer from particle-to-particle disintegration and the reversible capacity of the composites fades from the first cycle to the 34th by less than 50% [29].

Other kinds of metals such as zinc and aluminum [30] can also be coated onto the surface of graphite. The effects are
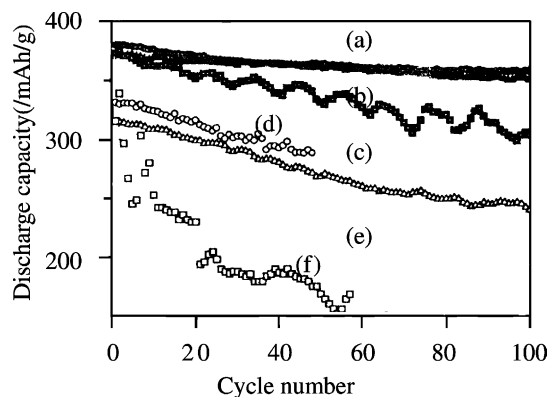

Fig. 2. Cycling performance of natural graphite (curves d, e and f) and Al-treated sample (curves a, b and c): circles, triangles and rectangles represent 0.2C, 0.5C and 1C rate, respectively (from [30]).

similar to the above mentioned. For example, due to decrease in charge-transfer resistance, the composite of Al and graphite shows marked improvement in cycling performance and rate capability as shown in Fig. 2 [30].

The metals discussed above usually form composites with carbon without much selectivity. When copper and silver are deposited onto the surface of graphite by dipping graphite into the aqueous solutions of their salts and following heat-treatment at 600 °C under argon atmosphere, the metals are selectively concentrated on the active sites at the graphite surface, and exist in metallic and carbidic forms to cover and/or remove these active sites. As a result, the composites absorb evidently less water when the electrode materials are built into cells under high humidity condition (about 1000 ppm H_2O), and show still good electrochemical performance though the virgin graphite exhibits good electrochemical behavior under low humidity condition only (<100 ppm H_2O) [31–33]. In addition, the deposited metals
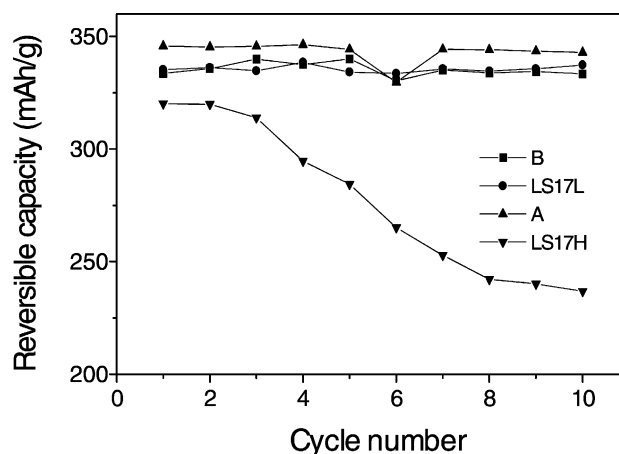

Fig. 3. Cycling behavior of natural graphite LS17 (curve LS17H) and the prepared composites of LS17 deposited with 10.2 wt.% Cu (curve A) and 8.6 wt.% Ag (curve B) when the anode materials were assembled into cells under high humidity condition (about 1000 ppm). For comparison, cycling behavior of LS17 under low humidity (below 100 ppm) is also shown as curve LS17L (excerpted from [33]).

contribute to reversible capacity. Typical results are shown in Fig. 3.

Oxides such as SnO [25], SnO$_2$ [34] and M$_x$O (M = Cu, Ni, Fe and Pb) [35] can also be coated onto graphitic carbon. For example, in the case of a composite of SnO with large surface-area synthetic graphite (KS6), it displays generally superior electrochemical performance relative to bulk SnO or the mechanical mixtures of KS6 and SnO of similar overall compositions such as reversible capacity, rate capability and cycle life. But their irreversible capacity loss in the first cycle is higher because of the required electro-reduction reaction to convert the oxide precursor into Sn-based Li storage compounds. Due to the presence of synergistic interaction between the two constituents SnO and graphite, the specific capacity of the composites is larger than that of the weighted one of SnO and graphite [25]. A composite of MCMB with tin oxide gives higher capacity than uncoated MCMB, but the capacity decreases with cycling due to severe volume changes of tin oxide. The cyclability can be improved by further coating copper on the surface of the composite since copper acts as an inactive matrix that provides a buffer against volume changes [34].

The reviewed results show that metals and metal oxides can act in several ways to improve electrochemical performance of graphitic carbon: (1) covering active sites at edge planes resulting in decrease of electrolyte decomposition, gas evolution, exfoliation and absorption of water in the presence of high humidity; (2) increasing conductivity leading to less charge-transfer resistance and improved high rate capability; and (3) acting as host for lithium storage leading to enhancement of reversible capacity. It should also be remembered that metal oxides usually present some unwelcome effects such as high irreversible capacity in the first cycle, which is an important factor that should be considered prior to practical application.

4. Coating by polymers and other kinds of carbon

In order to modify the surface structure of graphite and carbon anode materials, besides mild oxidation and deposition of metals and their oxides, polymers and other kinds of carbon can also be coated to achieve improved performance as anode materials.

4.1. Coating by polymers

At first, the polymers considered to coat on the carbon surface to improve its electrochemical performance of the composites are conductive and electroactive ones such as polythiophene [36], polypyrrole [37] and polyaniline [38]. Later, it was found that other kinds of polymers can also be used as effective coating.

Actions of polythiophene are multiple when it is coated onto the graphite (Lonza KS-44) surface [36]. At first, it acts as conductor since it is electronically conductive, and the

formed composite displays a good electric network. As a result, a pressing process can be omitted in the assembly line. Secondly, it can act as a binder, and additional insulating F-containing polymers are not necessary. Thirdly, lithium can also be doped therein although the reversible capacity is low, about 44 mAh/g, resulting in an increase of reversible capacity. At last, the polymer coating also decreases the contact of graphite with electrolyte and the consequent irreversible capacity [36].

When pyrrole is polymerized onto commercial SFG10 graphite by an in situ polymerization technique, the initial irreversible capacity is also decreased due to the reduction in the thickness of the formed SEI layer. A composite of PPy (7.8 wt.%) with graphite gives the optimum performance based on irreversible and reversible capacity. It possesses good reversibility, higher coulombic efficiency, good rate capability and better cycle life than the bare SFG10 graphite [37].

Different polyanilines such as emeraldine base, emeraldine salt and protonated polyaniline have been tried [38]. It was shown that they act as a binder and decrease the thickness of SEI film. As a result, capacity loss in the first cycle decreases [38].

Ionically conductive co-polymers can also be coated onto the surface of graphite acting to reduce the irreversible capacity and enhance the cycling life of natural graphite anode materials [39]. For example, an ionically conductive co-polymer can be encapsulated on the surface of natural graphite particles via radiation-initiated polymerization, and the composite shows great improvement in electrochemical performance including initial coulomb efficiency and cyclability in comparison with the virgin natural graphite. The improvement is due to the fact that encapsulation depresses the structural changes caused by the co-intercalation of solvated lithium ions and ensures a stable electrode impedance during the cycling [39].

Other polymers having no electro-activity (for example, polyelectrolytes like gelatin [38,40–42] and cellulose [38]) can also act to modify electrochemical performance of carbon anode materials.

When graphite particles are pretreated in an aqueous solution of gelatin, its molecules adsorb onto the particle surface as schematically illustrated in Fig. 4 [41] and present a significant impact on anode passivation as well as on the binding properties of the carbon particles, i.e. gelatin also serves as a binder and addition of special binder is not necessary [40,41]. The composite anode has lower irreversible loss (13–16%) than the classically prepared one (30–35%), and efficiency reaches values close to 100% in the third cycle. However, only when the concentration of gelatin solution used in the pre-treatment is high enough stable cycling can be achieved [40]. The reversible capacity of pretreated electrodes is just a little higher than that of conventional electrodes [38,40,41]. Cellulose presents the same effect [38]. The total content of the polyelectrolyte in the final anode is between 1 and 2 wt.%. The major effects
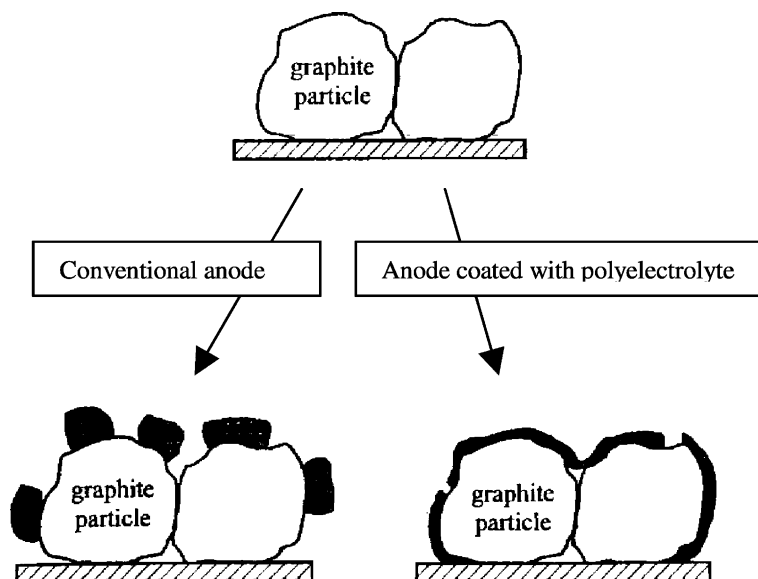
Fig. 4. A simple model about the coating actions of polyelectrolytes on graphite (from [41]).

and advantages of polyelectrolytes are: (1) no classical binder is required to prepare mechanically and electrochemically stable anodes, and (2) irreversible capacity in the first cycle is decreased probably due to formation of a more uniform passive film, whose growth is governed by the presence of polyelectrolyte molecules. The efficiency of polyelectrolyte pretreatment depends on the polyelectrolyte species, and the concentration, Bloom value, and pH of its solution for the pre-treatment procedure [38].

4.2. Coating with other kinds of carbons

In the case of graphitic carbon, PC is usually not regarded as an ideal electrolyte solvent because it decomposes at the graphite surface and an effective SEI film cannot be formed properly; it co-intercalates into graphite and results in exfoliation of graphene sheets. Therefore, EC-based electrolytes are commonly used. However, the melting point of PC ($-49\,^{\circ}$C) is lower than that of EC ($38\,^{\circ}$C) [1]. In order to broaden the application of liquid electrolyte-based lithium ion batteries, better performance at low temperature is a goal. Consequently, improving electrochemical performance of graphitic carbon for PC-based electrolyte by coating other kinds of carbons has become one focus. In the meanwhile, other kinds of improvements can also be achieved by this coating.

Carbon from thermal vapor decomposition at $1000\,^{\circ}$C is coated onto natural graphite [43,44]. When the graphite surface is completely coated by a carbon "shell", the PC content in the electrolyte with DMC can be up to 30 vol.% without decomposition of PC and exfoliation of graphite layers. The coated natural graphite shows much better electrochemical performance than "bare" natural graphite as anode material in both PC- and EC-based electrolytes [44]. By altering the scan rate during the measurement of cyclic voltammograms, both graphite "core" and carbon "shell" can be identified [43]. However, high pressure in the process of rolling and pressing should be avoided since it will destroy the coated carbon shell and expose the graphite surface to PC-based electrolyte again [43].

When artificial graphite (Lonza KS44) is dispersed in a tetrahydrofuran/acetone solution that contains coal tar pitch following heat-treatment of the loaded pitch at $1000\,^{\circ}$C in argon atmosphere, pores of <10 nm in the graphite are covered by the coke component resulting in a smaller surface-area than that of the pristine one. The reduction of surface-area of the coke-coated graphite leads to a decrease in the irreversible capacity in the first cycle, the extent of electrolyte (EC/DEC) decomposition, gas evolution and surface film growth in comparison with the virgin graphite electrode [45].

It is known that polymers can be precursors for carbon anode materials [1,2], and these kinds of carbons can also be coated onto graphite to avoid its direct contact with electrolytes. For example, carbon-coated graphite particles can be prepared by simple heat-treatment of mixtures of graphite and poly(vinyl chloride) at $800–1000\,^{\circ}$C in an argon flow. Since the turbostratic disordered carbon coating covers active edge sites of graphite and resists irreversible side-reactions such as electrolyte decomposition and graphite exfoliation, this coating suppresses the co-intercalation of solvated Li$^+$ and improves the initial charge–discharge coulombic efficiency, resulting in significant reduction of the initial irreversible capacity of the graphite in PC-based electrolyte. Nevertheless, this carbon coating greatly increases the specific surface-area of graphite particles [46]. In addition, compared with untreated graphite, reversible capacity and cycling behavior besides coulombic efficiency in the first cycle are markedly improved [46], which is different from the coke-coated one [45].

Since the coating is effective to improve electrochemical performance of the obtained graphite electrode, the analysis of the weight ratio of the carbon coating in the composite is important. It can be analyzed on the basis of thermal analysis by air oxidation, which is correlated with both the physical and electrochemical characteristics for a series of carbon-coated natural graphite [47], and the inverse of the density shows a linear relationship with carbon coating weight percentage in almost the whole range of carbon coating weight percentages.

In order to increase reversible capacity of carbon electrodes for lithium ion secondary batteries, coating by additional carbons is also an effective method. When coke carbon, a relatively cheap material, is modified with mesophase-pitch carbon by heat-treatment, the modified coke can have a reversible lithium capacity of 400 mAh/g while coke carbon powder and mesophase-pitch have only an initial reversible capacity of about 295 and 310 mAh/g between 0 and 1.5 V versus Li^+/Li, respectively [48]. Mesocarbon microbeads (MCMBs), which constitutes a promising carbon anode material, can also be coated with carbons from polymer precursors to achieve improvements [49]. For example, the surface coating of carbon from epoxy resin improves the electrochemical performance of the composite such as the charge–discharge capacity and cyclability. Nevertheless, the surface-area of MCMB also increases because of the formation of an amorphous epoxy resin coating layer [49].

In the case of low temperature carbon (amorphous carbon), though it has a high reversible capacity, there is a serious problem of low cyclability preventing its practical application. In order to improve the cycling behavior, amorphous carbon from epoxy or phenolic resin can be coated by impregnating it in resin solutions and a following heat-treatment of the mixture at temperatures below 900 °C [50]. Long cycle life for the composites can be achieved though the effects depend on the low temperature carbon species and resins.

In summary, the coating with polymers or other kinds of carbons can be an efficient method to improve electrochemical performance of carbon anode materials; the specific effects depend on the used polymers and deposited carbons. With the development of this coating, new and better carbon composite will be developed, for example graphite modified by coating with carbon and polymer from grafting, the compatibility of carbon anode materials with dry-type polymer is much improved [51].

5. Carbon nanotubes

As mentioned above, carbon anode materials are usually graphitic or amorphous carbons. Since the detection of carbon nanotubes in 1991 [52], they show some unique properties including potential use as anode materials of lithium ion batteries.

There are several classifications of carbon nanotubes. On the basis of configuration, it can be divided into three kinds of carbon nanotubes: armchair, zig-zag and chiral ones. On the basis of the degree of graphitization they can be divided into amorphous and graphitic ones. On the basis of structure or number of walls they can be classified into single wall and multiwall ones [53]. The following overview is based on the last classification.

5.1. Multiwall carbon nanotubes (MWNTs)

MWNTs consist of graphitic sheets rolled into closed concentric cylinders with a structure similar to that of Russian dolls. The concentric tubes are separated by van der Waals spacings of about 34 pm, a little larger than the interlayer distance of graphite, 33.5 pm. Their external diameters are on the order of nanometers and typical lengths are on the micrometer scale. They contain impurities and defects, whose amounts depend on preparation conditions. Most impurities such as catalysts particles, graphite and disordered carbons can be removed by purification. Defects such as dangling bonds, sidewall holes and open ends can be generally healed by annealing at high-temperature.

They can be prepared by two typical ways: catalytic decomposition of hydrocarbons such as acetylene [54], ethylene [57] and camphor vapor [58], or an electric arc technique [55]. Their electrochemical performance depends on their preparation process.

MWNTs produced by electric arc technique show an exfoliation of graphene layers when lithium intercalates using a 1 M $LiPF_6$ electrolyte dissolved in EC, PC and DMC (v/v/v = 1:1:3). Lithium intercalates between their graphene layers by formation of stage compound. However, *n*-stage compounds with n higher than 2 is not observed [55].

MWNTs prepared by catalytic decomposition without purification show high irreversible capacity. After purification and annealing, irreversible capacity decreases with annealing temperature [56].

Similar to the behavior of amorphous and graphitic carbon, the structure of MWNTs also play s a major role for both specific capacity and cycle life [57]. Slightly graphitized MWNTs exhibit a high specific capacity of 640 mAh/g during the first charge due to doping of lithium into regions without organized graphitic structure, micropores, edge sites and surfaces of graphitic layers. In contrast, well-graphitized MWNTs show a lower capacity of 282 mAh/g during the first charge. Both of them display an evident voltage hysteresis of about 1 V, which is higher than that of H-containing carbon. Perhaps, this is due to a longer diffusion distance for de-intercalating lithium. After 20 charge/discharge cycles, the charge capacity of the slightly graphitized MWNTs fades to 65.3% of their original charge capacity, but the well-graphitized MWNTs maintain 91.5% of their original charge capacity due to their stable structure [57].

Like the modification of other kinds of carbons by doping heteroatoms [59], carbon nanotubes can also be doped by
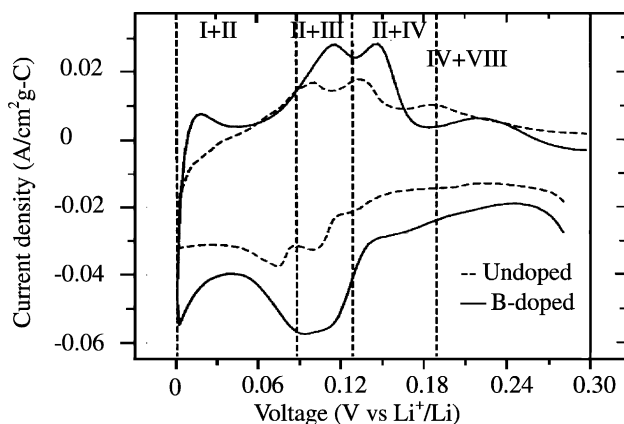
Fig. 5. Cyclic voltammograms of undoped and B-doped multiwall carbon nanotubes in the first cycle obtained at a sweep rate of 0.004 mV/s in 1 M LiClO$_4$ solution dissolved in EC/DEC (v/v = 1:1). The roman letters indicate the corresponding stage numbers (from [60]).

heteroatoms [60]. Boron-doped multiwall carbon nanotubes (B-MWNTs) consist of highly aligned ca. 35–45 graphene layers with good 3D ordering feature, and the boron doping destroys the local hexagonal symmetry. BC$_3$ nanodomains are observed and located either at the tips of the open ends or on the uppermost few layers of the B-MWNT. BET surface-areas of undoped and doped nanotubes are 10 and 12 cm^2/g, respectively, with almost similar mesopore volumes. Reversible capacity after doping increases from 156 to 180 mAh/g in the first cycle with almost equal coulomb efficiencies of 55–58%, which is from enhanced 3D ordering by B-doping. The coulomb efficiency increases to more than 92% after the second cycle. Highly reversible intercalation/de-intercalation of Li occurs with some undesirable reduction processes in the initial discharge process. The cycling behavior of both undoped and doped samples are quite satisfactory. Intercalation of lithium in these nanotubes takes place via staging transition, like in Li–graphite intercalation compounds as shown in Fig. 5 [60], which is a little different from the above-mentioned [55].

When carbon nanotubes are coated with a layer of copper oxide by electroless plating a layer of Cu following oxidation at 160 °C in air, they can reversibly store lithium up to 700 mAh/g since CuO in CuO/carbon nanotubes can reversibly store 268 mAh/g CuO. Li inserts into the CuO lattice at 1.7 to ~1.0 V and is released at 2.3 to ~2.5 V versus Li$^+$/Li according to the following equation [61]:

$$CuO + xe^- + xLi^+ \leftrightarrow CuOLi_x \tag{1}$$
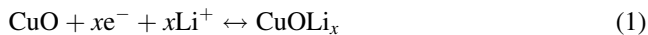
As mentioned above, carbon nanotubes can also be oxidized to effect an improvement of electrochemical properties. After oxidation with raw acid, the total discharge capacity (intercalation) during the first cycle is 660 mAh/g, and the reversible part is only 200 mAh/g. The nature of SEI film formed by reaction of surface groups on the carbon nanotubes with lithium upon discharge determines to a large extent the reversible and irreversible capacity of the carbon nanotubes. During oxidation in the mixture of acid, the residual acids play

an important role in this work and react with Li ion resulting in irreversible capacity. The H$_2$SO$_4$ and HNO$_3$ can easily permeate through the graphene sheets to make defects or pores in graphene sheets causing increase of reversible capacity [62].

5.2. Single wall nanotubes (SWNTs)

SWNTs can be envisioned as a single graphene sheet rolled into a cylinder with typical diameters in the range 1–2 nm and lengths of several micrometers. SWNTs of nearly uniform diameters self-organize into long crystalline "ropes" in which parallel nanotubes are also bound by van der Waals forces. The diameter of a rope is typically 10–50 nm corresponding to 30–600 tubes per rope. The number of tubes in a rope can range from 2–3 to several thousand. Like MWNTs they also contain impurities and defects. It has a high theoretical surface-area, and the total specific surface-area of the outside plane and the inside plane can be 2630 m^2/g. It can be prepared by thermal decomposition of CO under high pressure with catalysts, arc discharge or by laser ablation [63].

Lithium can reversibly intercalate into SWNTs, and the reversible capacities can range from 460 mAh/g, corresponding to a stoichiometry of Li$_{1.23}$C$_6$ [64], to 1000 mAh/g (Li$_{2.7}$C$_6$) after introduction of defects by ball milling [65]. However, irreversible capacity in the first cycle is very high, up to 1200 mAh/g ascribed to the large specific surface-area (350 m^2/g). From measurement of galvanostatic charge–discharge curves and cyclic voltammetry no well-defined redox potential for lithium insertion or removal in the nanotube lattice can be identified, ruling out the hypothesis of a stepwise mechanism via well-defined interstitial sites. Lithium can intercalate in the channels between nanotubes. This intercalation disrupts the intertube binding, analogous to exfoliation in layer hosts and different from the well-ordered staging of graphite. The disrupture leads to irreversible loss of crystallinity. Upon lithium intercalation, due to charge-transfer from lithium to carbon, resistance decreases continuously. Double layer capacitance effects are excluded from the contribution to high reversible capacity [64]. When ends of SWNTs are opened by concentrated acid, a composition of LiC$_6$ can be reached [66]. Elucidation of mechanistic details is still awaited though external surface and interior of the tubes can be additional sites for lithium residence.

In conclusion, carbon nanotubes display very interesting properties as anode materials. However, more studies and improvement are still needed. Since, they can be prepared in the form of thin films, they will be useful for the anode materials of promising microbatteries [67].

6. Concluding remarks

In summary, electrochemical performance of carbonaceous materials can be much improved. Mild oxidation can

remove reactive sites and/or defects in graphitic materials resulting in improvement of surface structure, formation of a dense layer of oxides acting as an efficient passivating film, and production of nanochannels/micropores for storage sites and passages for lithium. As a result, electrochemical performance including coulombic efficiency in the first cycle, reversible capacity and cycling behavior are improved. Metals and metal oxides can form composites with graphitic carbon, and they cover active sites at edge planes resulting in a decrease of electrolyte decomposition, gas evolution, exfoliation and absorption of water in the presence of high humidity, and an increase of conductivity leading to lower charge-transfer resistance and improved high rate capability; they can also act as hosts for lithium storage leading to an increased reversible capacity. The total effects also arrive at an improved electrochemical performance though the extent depends on the species of metals or metal oxides and the process. Coating by polymers can achieve several effects such as no need for fluorine-containing binder and conductive additives, less irreversible capacity loss and better cycling. Carbon coating can prevent the exposure of graphite or graphitic carbon core to electrolytes, and result in reduced electrolyte decomposition and exfoliation of graphene sheets, higher coulombic efficiency in the first cycle and improved cycling behavior. The newly explored carbon nanotubes also show interesting properties as anode materials for lithium ion batteries.

With the progressive application of novel technologies, other methods can also be employed to improve electrochemical performance of carbon anode materials. For example, irradiation by electron beam can increase reversible capacity in combination with reduction of the amount of binder and structural changes during cycling [68]. Plasma-assisted chemical vapor deposition can prepare flat and pinhole free carbon thin film making microbatteries as a promise for future use in microelectronics [69]. Graphite surface can also be modified by silylation in nonaqueous solution due to coupling of silane with hydroxyl-containing carbon surface species such as hydroxyl-groups to reduce irreversible capacity loss [70]. Formation of hybrid carbon such as that of graphite and hard carbon can be promising anode material for long-life lithium ion batteries [71,72]. The effects of heteroatoms such as boron [73] and sulfur [74] will be explored in more detail and thus unwelcome effects from doping with heteroatoms will be avoided as much as possible and the favorable effects can be fully utilized. Of course, carbonaceous materials can also be applied to prepare other kinds of anode materials such as SnO to reduce irreversible capacity and improve cycling performance [75]. Mild milling can be a good method to improve reversible capacity and coulomb efficiency in the first cycle of graphite [76]. In the near future, composite carbon anode materials superior to the current dominant commercial product MCMB will come into use [77].

References

[1] Y.P. Wu, C. Wan, C. Jiang, S.B. Fang, Principles, Introduction & Advances of Lithium Secondary Batteries, Tsinghua University Press, Beijing, 2002.

[2] M. Winter, J.O. Besenhard, Lithiated carbon, in: J.O. Besenhard (Ed.), Handbook of Battery Materials, Weinheim, Wiley-VCH, 1999, p. 383.

[3] M. Noel, R. Santhanam, J. Power Sources 72 (1998) 53.

[4] E. Peled, C. Menachem, A. Melman, J. Electrochem. Soc. 143 (1996) L4.

[5] Y.P. Wu, C. Wan, C. Jiang, S.B. Fang, Y.Y. Jiang, Carbon 37 (1999) 1901.

[6] T. Nakajima, K. Yanagida, Tanso 174 (1996) 195.

[7] Y.P. Wu, C. Jiang, C. Wan, J. Li, Chin. J. Batteries 30 (2000) 143.

[8] Y.P. Wu, C. Jiang, C. Wan, R. Holze, Solid State Ionics 156 (2003) 283.

[9] C. Menachem, Y. Wang, J. Floners, E. Peled, S.G. Greenbaum, J. Power Sources 76 (1998) 180.

[10] H. Buqa, P. Golob, M. Winter, J.O. Besenhard, J. Power Sources 97/98 (2001) 122.

[11] Y.P. Wu, C.Y. Jiang, C.R. Wan, E. Tsuchida, Electrochem. Commun. 2 (2000) 272.

[12] M.E. Spahr, H. Wilhelm, F. Joho, J. Panitz, J. Wambach, P. Novák, N. Dupont-Pavlovsky, J. Electrochem. Soc. 149 (2002) A960.

[13] Y. Ein-Eli, V.R. Koch, J. Electrochem. Soc. 144 (1997) 2968.

[14] Y.P. Wu, R. Holze, in: Extended Abstracts of the 53rd Meeting of International Society of Electrochemistry, Düsseldorf, Germany, September 15–20, 2002.

[15] Y.P. Wu, C. Jiang, C. Wan, R. Holze, J. Appl. Electrochem. 32 (2002) 1011.

[16] Y.P. Wu, C. Jiang, C. Wan, R. Holze, J. Power Sources 111 (2002) 329.

[17] Y.P. Wu, C. Jiang, C. Wan, E. Tsuchida, J. Mater. Chem. 11 (2001) 1233.

[18] Y.P. Wu, C. Jiang, C. Wan, R. Holze, Electrochem. Commun. 4 (2002) 483.

[19] H. Momose, H. Honbo, S. Takeuchi, K. Nishimura, T. Horiba, Y. Muranaka, Y. Kozono, J. Power Sources 68 (1997) 208.

[20] K. Nishimura, H. Honbo, S. Takeuchi, T. Horiba, M. Oda, M. Koseki, Y. Muranaka, Y. Kozono, H. Miyadaera, J. Power Sources 68 (1997) 436.

[21] P. Yu, J.A. Ritter, R.E. White, B.N. Popov, J. Electrochem. Soc. 147 (2000) 1280.

[22] P. Yu, J.A. Ritter, R.E. White, B.N. Popov, J. Electrochem. Soc. 147 (2000) 2081.

[23] L. Shi, Q. Wang, H. Li, Z. Wang, X. Huang, L. Chen, J. Power Sources 102 (2001) 67.

[24] T. Takamura, K. Sumiya, J. Suzuki, C. Yamada, K. Sekine, J. Power Sources 81/82 (1999) 368.

[25] J. Lee, R. Zhang, Z. Liu, J. Power Sources 90 (2000) 70.

[26] B. Veeraraghavan, A. Durairajan, B. Haran, B. Popov, R. Guidotti, J. Electrochem. Soc. 149 (2002) A675.

[27] M. Egashira, H. Takatsuji, S. Okada, J. Yamaki, J. Power Sources 107 (2002) 56.

[28] L. Shi, H. Li, Z. Wang, X. Huang, L. Chen, J. Mater. Chem. 11 (2001) 1502.

[29] A. Ulus, Y. Rosenberg, L. Burstein, E. Peled, J. Electrochem. Soc. 149 (2002) A635.

[30] S. Kim, Y. Kadoma, H. Ikuta, Y. Uchimoto, M. Wakihara, Electrochem. Solid State Lett. 4 (2001) A109.

[31] Y.P. Wu, C. Wan, C. Jiang, E. Tsuchida, Electrochem. Commun. 2 (2000) 626.

[32] Y.P. Wu, C. Jiang, C. Wan, R. Holze, J. Power Sources 112 (2002) 255.

[33] Y.P. Wu, C. Jiang, C. Wan, R. Holze, Carbon, in press.

[34] J.K. Lee, D.H. Ryu, J.B. Ju, Y.G. Shul, B.W. Cho, D. Park, J. Power Sources 107 (2002) 90.

[35] H. Huang, E.M. Kelder, J. Schoonman, J. Power Sources 97/98 (2001) 114.

[36] S. Kuwabata, N. Tsumura, S. Goda, C.R. Martin, H. Yoneyama, J. Electrochem. Soc. 145 (1998) 1415.

[37] B. Veeraraghavan, J. Paul, B. Haran, B. Popov, J. Power Sources 109 (2002) 377.

[38] M. Gaberscek, M. Bele, J. Drofenik, R. Dominko, S. Pejovnik, J. Power Sources 97/98 (2001) 67.

[39] Q. Pan, K.K. Guo, L.Z. Wang, S.B. Fang, Solid State Ionics 149 (2002) 193.

[40] J. Drofenik, M. Gaberscek, R. Dominko, M. Bele, S. Pejovnik, J. Power Sources 94 (2001) 97.

[41] M. Gaberscek, M. Bele, J. Drofenik, R. Dominko, S. Pejovnika, Electrochem. Solid State Lett. 3 (2000) 171.

[42] M. Bele, M. Gaberscek, R. Dominko, J. Drofenik, K. Zupan, P. Komac, K. Kocevar, I. Musevic, S. Pejovnik, Carbon 40 (2002) 1117.

[43] H. Wang, M. Yoshio, J. Power Sources 93 (2001) 123.

[44] M. Yoshio, H. Wang, K. Fukuda, Y. Hara, Y. Adachi, J. Electrochem. Soc. 147 (2000) 1245.

[45] S. Yoon, H. Kim, S.M. Oh, J. Power Sources 94 (2001) 68.

[46] H. Lee, J. Baek, S. Jang, S. Lee, S. Hong, K. Lee, M. Kim, J. Power Sources 101 (2001) 206.

[47] H. Wang, M. Yoshio, T. Abe, Z. Ogumi, J. Electrochem. Soc. 149 (2002) A499.

[48] Y. Sato, Y. Kikuchi, T. Nakano, G. Okuno, K. Kobayakawa, T. Kawai, A. Yokoyama, J. Power Sources 81/82 (1999) 182.

[49] J.S. Kim, W.Y. Yoon, K.S. Yoo, G. Park, C.W. Lee, Y. Murakami, D. Shindo, J. Power Sources 104 (2002) 175.

[50] M. Saito, K. Yamaguchi, K. Sekine, T. Takamura, Solid State Ionics 135 (2000) 199.

[51] T. Tsumura, A. Katanosaka, I. Soumaa, T. Ono, Y. Aihara, J. Kuratomi, M. Inagaki, Solid State Ionics 135 (2000) 209.

[52] S. Iijima, Nature 354 (1991) 56.

[53] Y.P. Wu, E. Rahm, R. Holze, Chin. J. Batteries (Dianchi) 32 (2002) 356.

[54] V.A. Nalimova, D.E. Sklovsky, N. Bondarenko, H. Alvergnat-Gaucher, S. Bonnamy, F. Beguin, Synth. Met. 88 (1997) 89.

[55] G. Maurina, Ch. Bousqueta, F. Henna, P. Bernier, R. Almairac, B. Simon, Solid State Ionics 136/137 (2000) 1295.

[56] F. Leroux, K. Méténier, S. Gautier, E. Frackowiak, S. Bonnamy, F. Beguin, J. Power Sources 81/82 (1999) 317.

[57] G. Wu, C.S. Wang, X.B. Zhang, H.S. Yang, Z. Qi, P. He, W. Li, J. Electrochem. Soc. 146 (1999) 1696.

[58] M. Sharon, W.H. Hsu, H.W. Kroto, D. Walton, A. Kawahara, T. Ishihara, Y. Takita, J. Power Sources 104 (2002) 148.

[59] Y.P. Wu, E. Rahm, R. Holze, Electrochim. Acta 47 (2002) 3491.

[60] I. Mukhopadhyay, N. Hoshino, S. Kawasaki, F. Okino, W.K. Hsu, H. Touhara, J. Electrochem. Soc. 149 (2002) A39.

[61] G.T. Wu, C.S. Wang, X.B. Zhang, H.S. Yang, Z.F. Qi, W.Z. Li, J. Power Sources 75 (1998) 175.

[62] Z. Yang, H. Wu, B. Simard, Electrochem. Commun. 4 (2002) 574.

[63] S. Shiraishi, H. Kurihara, K. Okabe, D. Hulicova, A. Oya, Electrochem. Commun. 4 (2002) 593.

[64] A. Claye, J.E. Fischer, C.B. Huffman, A.G. Rinzler, R.E. Smalley, J. Electrochem. Soc. 147 (2000) 2845.

[65] B. Gao, C. Bower, J.D. Lorentzen, L. Fleming, A. Kleinhammes, X.P. Tang, L.E. McNeil, Y. Wu, O. Zhou, Chem. Phys. Lett. 327 (2000) 69.

[66] E. Jouguelet, C. Mathis, P. Petit, Chem. Phys. Lett. 318 (2000) 561.

[67] Y.P. Wu, E. Rahm, R. Holze, Chin. J. Batteries (Dianchi) 33 (2003) 47.

[68] E. Endo, T. Kihira, S. Yamada, H. Imoto, K. Sekai, J. Power Sources 93 (2001) 215.

[69] T. Fukutsuka, T. Abe, M. Inaba, Z. Ogumi, J. Electrochem. Soc. 149 (2002) A1260.

[70] H. Buqa, C. Grogger, M.V. Alvarez, J.O. Besenhard, M. Winter, J. Power Sources 97/98 (2001) 126.

[71] K. Yanagida, A. Yanai, Y. Kida, A. Funahashi, T. Nohma, I. Yonezu, J. Electrochem. Soc. 149 (2002) A804.

[72] Y. Kida, K. Yanagida, A. Funahashi, T. Nohma, I. Yonezu, J. Power Sources 94 (2001) 74.

[73] C. Kim, T. Fujino, T. Hayashi, M. Endo, M.S. Dresselhaus, J. Electrochem. Soc. 147 (2000) 1265.

[74] Y.P. Wu, S.B. Fang, Y.Y. Jiang, R. Holze, J. Power Sources 108 (2002) 245.

[75] H. Li, X. Huang, L. Chen, J. Power Sources 81/82 (1999) 335.

[76] C. Natarajan, H. Fujimoto, A. Mabuchi, K. Tokumitsu, T. Kasuh, J. Power Sources 92 (2001) 187.

[77] S. Hossain, Y. Saleh, R. Loutfy, J. Power Sources 96 (2001) 5.